Proceedings of the ASME 2012 International Mechanical Engineering Congress & Exposition
IMECE2012
November 9-15, 2012, Houston, Texas, USA

IMECE2012-87345

OPTIMIZATION OF INDUCTION HARDENED AISI 1040 STEEL BY EXPERIMENTAL DESIGN METHOD AND MATERIAL CHARACTERIZATION ANALYSIS

Mert Onan
Kocaeli University
Kocaeli, Turkey
H.İbrahim Ünal
Kocaeli University
Kocaeli, Turkey
Kasım Baynal
Kocaeli University
Kocaeli, Turkey
Furkan Katre
Katre Induction Hardening Company
Kocaeli, Turkey

ABSTRACT

Nowadays, some of the steel parts have been applied induction hardening for better mechanical properties in the automotive and aerospace industry sectors. Induction hardening is commonly used in steels, are high magnetic permeability. Martensite formation was observed application as a result of non-diffusion transformation after induction hardening. At this period, there were chosen three factor such as power supplied, scan rate, distance between work piece and coil, were affected material properties. Developed response variables such as surface hardness and case depth were determined after the experiments were done in the industrial conditions. In this study, data were taken by Taguchi method using L27 experiment orthogonal arrays table. Analysis of Variance (ANOVA) was employed with the help of data taken and regression equation was determined. As a result of these experiments and analyses, the optimization of the process conditions for induction hardened steel was investigated. As a consequence of the optimization, microstructural characterization using Light microscopy was carried out to determine the effects of the hardness from the outer surface to the center and nevertheless transformations associated with structural changes are investigated and so that results are determined.

Keywords: Induction hardening, Taguchi method, Microstructural characterization, Phase transformation

INTRODUCTION

Induction hardening carried out on an induction hardening machine consist of a series of heat treatment processes; optional pre-heating, heating, quenching and tempering. Case hardening allows the surface to be hard for strength or protection against wear but allows the core to remain soft, providing ductility and resistance to cracking. A wide variety range of material including carbon steels, martensitic stainless steel, gray cast iron can be induction hardened, containing generally with carbon content 0,2 % to 0,6% and alloy elements containing steel are sometimes suitable commonly. Both carbon and alloy steels with normalized and annealed structures can be induction hardened but they require longer heating cycles and quench times, increasing the chances of cracking. Additionally, steels with a carbon content greater than 0,5% are susceptible to cracking, as well as higher-alloy materials [1]. Many methods of induction hardening may be applied but spin hardening uses a circular inductor and contains heating equipment with sufficient coil numbers for heating steel parts generally [2]. To predict against the effects of near-equilibrium cooling, spray cooling system using a polymer based quenching were used so that hard phases such as martensite occurred. The maximum expected surface hardness after induction hardening would be approximately 55 HRc [3], therefore case depth limits of 2 mm to 5 mm were deemed acceptable [4]. These conditions resulted in a successful hardening process. To obtain an adequate surface hardness and case depth, the process parameters were changed according to the choice of material. Induction hardening was performed according to the following formula [5]:

$$\delta = \sqrt{\frac{\rho}{\pi \mu f}} \qquad (1)$$

The magnetic permeability of the ferromagnetic materials strongly depends on the composition of the materials and on the ambient conditions (such as temperature, magnetic field intensity and saturation) [5].

EXPERIMENTAL DESIGN

Although ISO standards are related to the aspects of customer and employee satisfaction, ISO quality standards contain the

Copyright © 2012 by ASME

basic statistical approach to process parameter and variable control during a surface hardening or heat treatment process [6,7]. Different surface layers (0,2 mm to 10 mm) are created on work pieces, made of steel hardened by the induction hardening process. The most important characteristics of the material hardening process are the hardness value and also the case depth lead to show effect of hardness [8,9]. Optimization studies examined the distance between the coil and the material, applied power, frequency, current, scan rate, cooling time, quench flow and time as variables affecting the parameters [9,10,11].

In this study, AISI 1040 medium carbon steel was selected and induction hardened by using different parameters such as power supplied, scan rate, distance between work piece and coil. Optimization studies conducted to evaluate the effect of these process variables in induction hardening on the attainable hardness and case depth. Such as experimental design, Taguchi's L27 orthogonal array have been adopted to evaluate experiments in induction hardening processes. Developed response variables such as surface hardness and case depth were determined after the experiments were performed in the industrial conditions. Analysis of variance (ANOVA) was employed with the help of data's taken and a general regression was applied. The value of adjusted S/N ratio were intended to be as large as possible, and the results of the surface hardness and case depth were defined differently respectively. As a result of the optimization, the percent of the S/N ratio 60% surface hardness and 40% case depth were calculated, also results were used for investigation of material structural transformation. Material characterization were carried out by light microscopy and different structures such as martensite, pearlite and ferrite were observed. The influences of process factor and level variation on the microstructure were discussed.

MATERIAL AND METHOD

The induction hardening process were done at different conditions which was given in Table 2. The investigation was performed on cylindrical samples made of medium carbon steel corresponding to AISI 1040. The cylinders were machined to the specified dimensions of 10 cm length and 4 cm diameter by a lathing process. The chemical composition of AISI 1040 steel is given in Table 1.

Table 1. The chemical composition of AISI 1040 steel

Material Composition	**C (%)**	**Si (%)**	**Mn (%)**	**P_{max} (%)**	**S_{max} (%)**	**Fe**
AISI 1040	0,37-0,44	0,15-0,35	0,60-0,90	0,040	0,050	Balance

After induction hardening treatment, surface hardness were measured on the AISI 1040 steel surfaces through a line at the Rockwell hardness tester. Additionly, cylindrical samples were cut from the middle of material for investigation case depth. Also microstructural characterization were done from these surfaces.

Some of the AISI 1040 cylinder samples cut from the middle of the material had heights of 2 cm and radii of 4 cm. These surfaces were prepared for metallographic examination. Grinding was carried out with 120, 320, 600 and 1000 grit size SiC abrasive papers, and the surfaces were then polished with 3 μm diamond paste. Micro-hardness values were measured from the polished surfaces using a Zwick model 3132 hardness tester. After the micro-hardness measurements were performed, the surfaces were etched with 3% Nital to obtain good phase contrast. The etched specimens were investigated under using a Zeiss Axiotech 100 model light microscope.

EXPERMENT DESIGN APPLICATION

After the non-controlled and controlled process variable parameters were discussed with the sector employees, the power supplied, scan rate and distance between work piece and coil were determined to be controlled parameters and a cause-result diagram of induction hardening process was created. Randomization was applied to the experiments, and levels of factors that would give correct results were obtained. An L27 orthogonal experiment design was chosen for the factors and the levels used are given in Table 2.

Table 2. L27 orthogonal experiment design factors

Factors	**Factor description**	**Level 1**	**Level 2**	**Level 3**
Power ratio	P	0.2	0.5	0.7
Scan rate (mm/s)	S	2,5	5	7,5
Coil and work piece distance (mm)	G	4	8	12

From these experiments, a mathematical model was subsequently generated and was given below;

$$Y_{ijkl} = \mu + P_i + S_j + G_k + PS_{ij} + PG_{ik} + \ldots \\ \ldots + SG_{jk} + PSG_{ijk} + \varepsilon_{ijk} \quad (2)$$

After Taguchi's L27 orthogonal array had been adopted to evaluate experiments in induction hardening processes, the resulting surface hardness and case depth were measured and they were analyzed by Minitab software separately. According to the results, the ratio between the surface hardness and case depth was determined to be 60% effective surface hardness and 40% case depth.

Induction hardened steel is fabricated with variable surface hardness's, according to the specification that these steels should be hardened for either high strength or wear. As a result, the S/N ratios from the surface hardness and hardness depth were calculated and then corrected using the "largest is the best" method, with the results being given statistically.

Copyright © 2012 by ASME

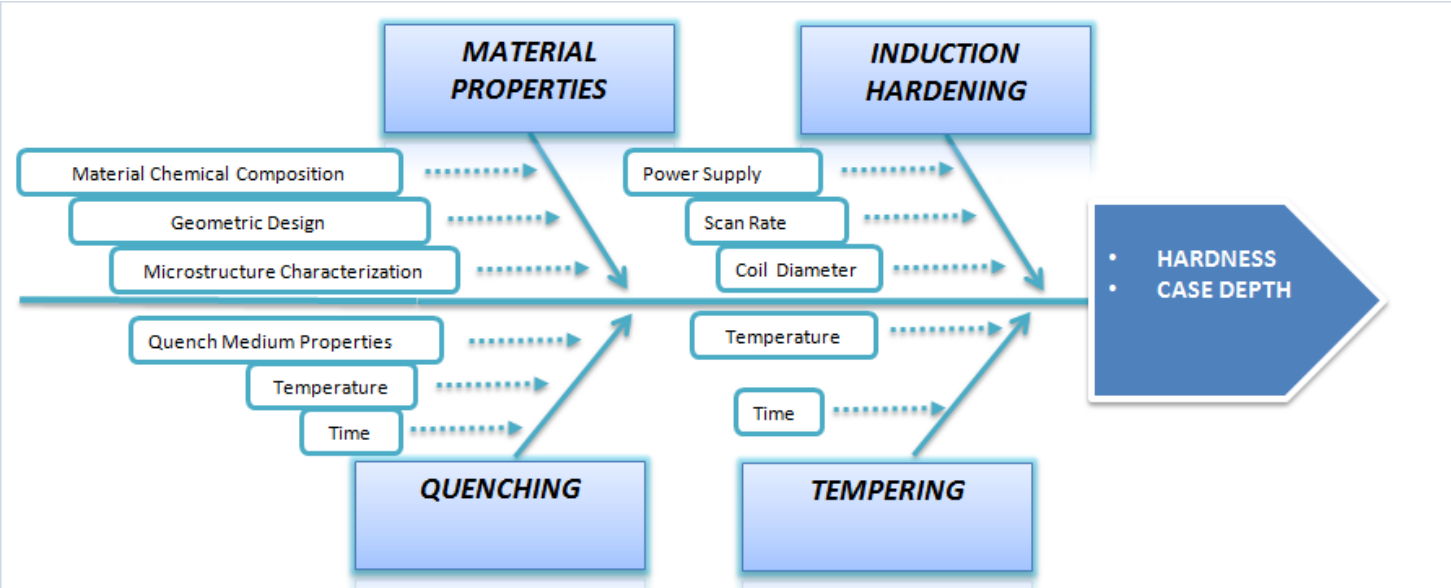


Figure 1. Induction hardening process cause-result diagram

RESULTS AND CONCLUSION

The results of induction hardening focusing on the material and conditions are seen in Figure 1. Considering parameters were determined on the results of induction hardening. But the quenching conditions were taken as constant and tempering was not necessary for AISI 1040 steel especially.

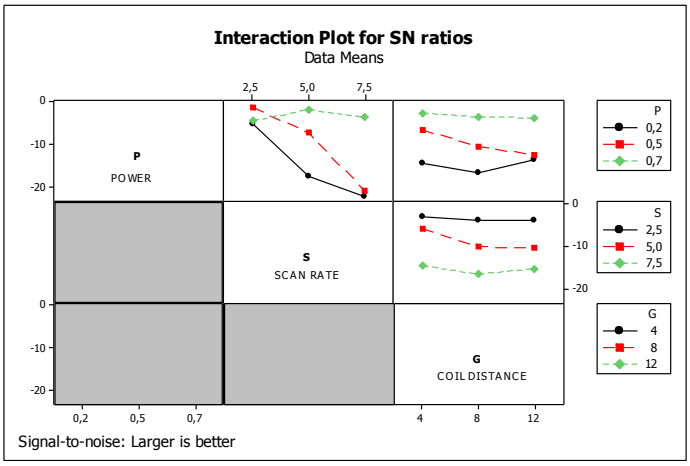


Figure 2. Interaction Plot for S/N ratios

The interactions between the adjusted results of the factor changes around the different levels are given in the interaction plot table using the S/N ratio, derived using the "larger is better" method, were generated according to formula below [12];

$$SN_i = -10 \log \left[\frac{1}{N_i} \sum_{u=1}^{N_i} \frac{1}{y_u^2} \right] \qquad (3)$$

When G was constant, the results showed that the values for the

Table 3. Experimental design application results consist of surface hardness and adjusted case depth

	P	S	G	Hardness (HRc)	Standart Dev. of Hardness	Adj. Case Depth (mm)	S/N ratio of Adj. Case Depth
1	0,2	2,5	4	41,83	4,222	3,5	10,88
2	0,2	2,5	8	33,25	1,458	2	6,02
3	0,2	2,5	12	35,33	4,037	1	0,00
4	0,2	5	4	15,08	12,795	0,3	-10,46
5	0,2	5	8	8,67	3,758	0,1	-20,00
6	0,2	5	12	11,58	0,274	0,1	-20,00
7	0,2	7,5	4	3,92	1,823	0,1	-20,00
8	0,2	7,5	8	5,25	3,029	0,1	-20,00
9	0,2	7,5	12	13,50	1,432	0,1	-20,00
10	0,5	2,5	4	39,33	2,408	5	13,98
11	0,5	2,5	8	49,67	1,084	4,5	13,06
12	0,5	2,5	12	51,25	1,565	4	12,04
13	0,5	5	4	49,08	1,643	3	9,54
14	0,5	5	8	25,08	3,546	1,5	3,52
15	0,5	5	12	21,67	12,877	0,5	-6,02
16	0,5	7,5	4	13,83	2,903	0,2	-13,98
17	0,5	7,5	8	6,42	1,673	0,1	-20,00
18	0,5	7,5	12	4,67	1,817	0,1	-20,00
19	0,7	2,5	4	46,92	2,588	1	0,00
20	0,7	2,5	8	45,67	0,570	1	0,00
21	0,7	2,5	12	52,33	2,043	1	0,00
22	0,7	5	4	55,42	1,140	4,2	12,04
23	0,7	5	8	45,92	4,022	3,5	10,88
24	0,7	5	12	48,33	1,275	3	9,54
25	0,7	7,5	4	53,17	0,962	2,5	7,96
26	0,7	7,5	8	45,50	3,493	2,2	6,85
27	0,7	7,5	12	39,17	5,805	1,8	5,11

Copyright © 2012 by ASME

power and scan rate were ratios of selected 0,7 and 5 cm/s, respectively, to achieve the best induction hardening of the material. When S was constant, the results were significantly different between power at ratios of 0,2-0,5-0,7. a P value ratio of 0,7 and a 4 mm distance between the coil and the work piece gave the best S/N ratio results. Additionally, it is considered important to shift to lower S/N ratios, which were shown to significantly reduce effective induction hardening with controlling power at ratios of 0,2 and 0,5. When P was constant, there was no intersection between the lines and no correlation was found between the factors in the data obtained from these experiments on the Figure 2.

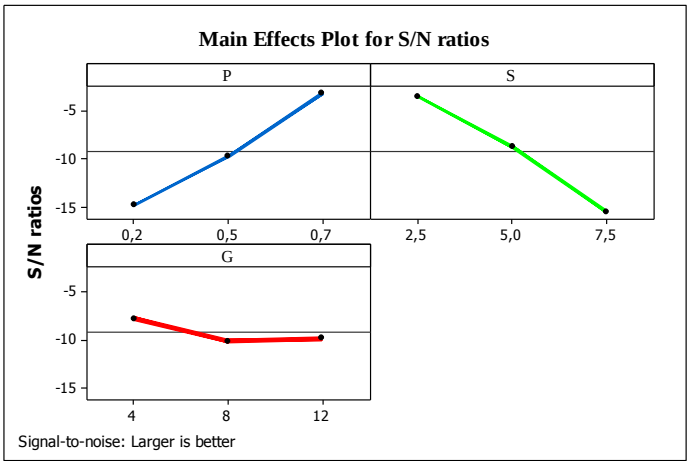


Figure 3. The optimum S/N results for each factor separately analyzed by Minitab software

The optimum results from the experiments are a power value ratio of 0,7, a scan rate value of 2,5 mm/s and a distance between the coil and the work piece of 4 mm separately, as shown on the Figure 3.

$$F = \frac{\text{Variance explained by factors}}{\text{Unexplained variance}} = \frac{MS treatment}{MS error} \quad (4)$$

After the formulation of the hypothesis, the results were compared according to the above F test formula [13] for each factor and interaction. Fraction of the mean square of factors and intersections to the mean square error was given F value. Statistical and the F test results are given in Table 4.

Table 4. Results contains Adj. Sum Square (SS), Adj. Mean Square (MS) and F test results

Source	DF	Seq SS	Adj SS	Adj MS	F
P	2	602,36	602,36	301,18	30,03
S	2	639,43	639,43	319,72	31,88
G	2	28,63	28,63	14,31	1,43
P*S	4	435,74	435,74	108,94	10,86
P*G	4	40,56	40,56	10,14	1,01
S*G	4	16,66	16,66	4,16	0,42
Error	8	80,23	80,23	10,03	
Total	26	1843,61			
S = 3,16687		R-Sq = 95,65%		R-Sq(adj) = 85,86%	

The hypothesis regarding to hardening process (relation of heating-quenching-hardening) using equation 3 and 4 are tested.

H1 : $P_i = 0$, (Power ratio is effective over hardening process and results of material hardness or case depth)
F = 30,03/10,03 = 2,99 $F_{2,8}$ = 2,81 (α= 0,10) (5)

H2 : Sj = 0 (Scan rate is effective over hardening process and results especially)
F = 31,88/10,03 = 3,17 $F_{2,8}$ = 2,81 (α= 0,10) (6)

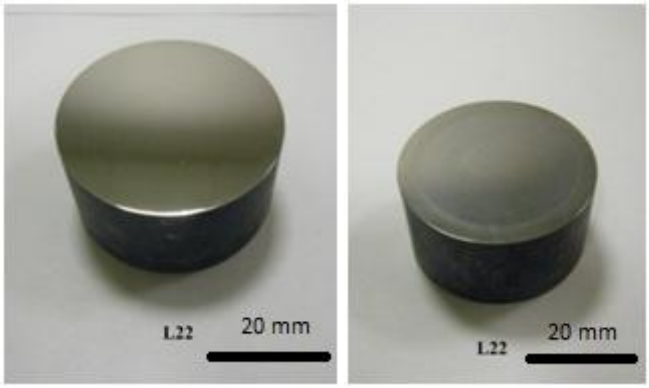
H3 : $G_k = 0$ (Coil distance to work piece is not effective than other parameters)
F = 1,43/10,03 = 0,14 $F_{2,8}$ = 2,81 (α= 0,10) (7)

H4 : $PS_ij = 0$ (Interaction between power ratio and scan rate is more effective than other interactions)
F = 10,86/10,03 = 1,08 $F_{4,8}$ = 3,11 (α= 0,10) (8)

The hypothesis can't be accepted H1, H2 and H4 respectively. But H3 can be accepted a little impact between coil distance and work piece because of selected wide range coil distance. The interaction of power ratio and scan rate have significant impacts on the results.

Regression equation results according to S/N ratios of total impact of case depth and surface hardness as an number between 0 and 1 were obtained, the induction hardening process conditions will be effective near to 1, it can be calculated as a result of regression equation. And condition of interlevel results will be calculated from regression equation.

$$Regression\ Equation = 24{,}39 - 41{,}83\ x\ P - 8{,}95\ x\ S - 2{,}16\ x\ G + 14{,}00\ x\ PxS + 4{,}03\ x\ PxG + 0{,}44\ x\ SxG - 0{,}94\ x\ PxSxG \quad (9)$$



(a) (b)

Figure 4. Metallographic preparation of induction hardened AISI 1040 steel a) Grinding and polished surface b) %3 nital etched surface

Copyright © 2012 by ASME

After grinding and polishing surface were seen like an mirror (Figure 4a) and then sun corona phenomena was observed on the induction hardened AISI 1040 steel surface, explained material grey color changes on the induction hardened layer from surface to core of material, was seen on the Figure 4b.

Samples are the same view compared to surface hardened steel similarly.

hardness value, decreasing from the surface to the core, reaches 37 HRc at this zone. Considering the micro hardness evaluations, the effective case depth is determined to be 2,8 mm. The increase of the ferrite grain size at the inner regions, is given in Figure 5c. Ferrite such as like white regions and perlite such as like dark side regions were observed on the Figure 5c. Total hardness case depth was ended at the 4,2 mm along the surface. Hardness lower structure such as ferrite and perlite were found at the nearest zone of the center and were

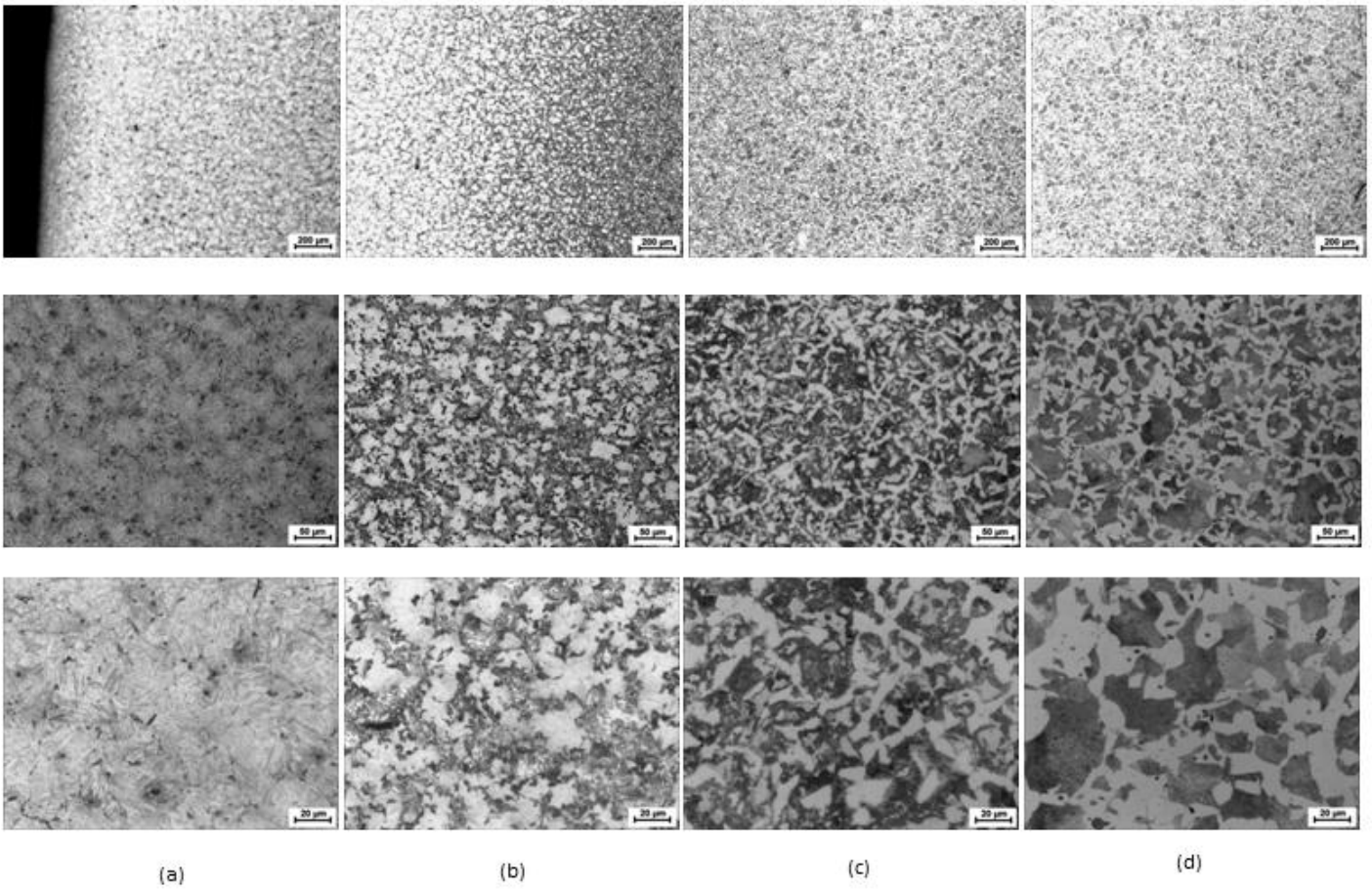


Figure 5. Comparision of four stage between surface to core microstructural changes on AISI 1040 steel acording to production parameters L22, 0,7/5/4, %3 nital etched, a) Surface b) Transformation zone c) Middle d) Center (x05,x20,x50)

Microstructural characterization from surface to core along 6 mm is done for the L22 experiment specimen giving the optimum value as a result of the optimization using the hardness and case depth. Structural changes were observed in the studies made starting from the surface towards the center at four stages on the Figure 5. Lata type martensite structure, increasing the surface hardness and occurring fully at surface, can be seen at Figure 5a. From Figure 5b, the microstructure spectrum of the transition zone, where the martensitic formation does not occur completely and there is some retained austenite in the structure, can be observed . The observed on the Figure 5d. Because of scan rate were 5 mm/s at the L22 conditions during induction hardening process, according to heating and quenching of near to core zone were not applied effectively. As a result of induction hardening, formation of ferrite and perlite were seen in evidence clearly at the core zone.

CONCLUSION

The optimization studies of induction hardening were performed and hardness and case depth were measured and analyzed.

- When the results was compared, an optimal result were given in the $P_3S_2G_1$ experimental design.
- According to F test results, power ratio, scan rate and intersections were more effective than other factors.

Copyright © 2012 by ASME

- The selection of higher power ratio and lower scan rate affected micro structural transformation during hardening process. As a result of applying higher power ratio or lower scan rate, induction hardening allowed high surface hardness.
- An hard phase, called martensite, were not 100% observed on the Light microscopy.
- Micro structural characterization showed that four different region from surface to inner surface, was called martensite, perlite and ferrite respectively.

ACKNOWLEDGMENTS

For applying induction hardening to steel materials were provided from Sadem steel and iron company sale department in Kocaeli. Special thanks to Induction Hardening company member mechanical engineer Furkan Katre for helping experimental process. About resulting the project, special thanks to undergraduate students Orkun Kaan Balkan and Hilal Gencer at different part of study such as cutting of metal and metallographic specimen preparation.

NOMENCLATURE

ρ :resistivity (Ohm m)
μ :magnetic permeability ($^{H}/_{m}$)
f :frequency (Hz)
δ: Case (penetration)depth(mm)

REFERENCES

[1] Davis, J.R., 2005, "Gear materials, properties, and manufacture", ASM International, Ohio, 2005.
[2] Wai, H.P.,Aung, S.S., and Win T., 2008, "Work Coil Design used in Induction Hardening Machine", World Academy of Science, Engineering and Technology, 42.
[3] Ralkhit, A.K., "Heat Treatment of Gears: A Practical Guide for Engineers", ASM International, US, Chap. 9.
[4] Modern Metal cutting, 1996, Sandvik Handbook.
[5] Callebout J., 2007, "Induction Heating, Power Quality & Utilisation Guide", Section 7.
[6] Vaxevanıdıs, N.M., 2006, "An Overvıew And A Comparıson Of Iso 9000:2000 Qualıty System Standards Wıth Related Automotıve Ones (QS9000, ISO/TS 16949) And TQM Models (MBNQA And EFQM)", Annals Of The Faculty Of Engıneerıng Hunedoara, Tome Iv, Fascicole 2.
[7] "TS ISO/TS 16949: Quality management systems – Particular requirements for the application of ISO 9001:2000 for automotive production and relevant service part organizations", 2005.
[8] Bodart, O., Bourean, A.V., Touzani, R., 2001, "Numerical investigation of optimal control of induction heating process", Applied Mathematical Model, 25, pp. 697–712.
[9] Palaniradja, K., Alagumurthi, N., and Soundararajan, V., 2010, "Hardness and Case Depth Analysis Through Optimization Techniques in Surface Hardening Processes", The Open Materials Science Journal, 4, pp. 38-63.
[10] Kayacan, M.C., 2004, "A fuzzy approach for induction hardening parameter selection", J. Materials and Design, 25 (2), pp. 155–161.
[11] Kohli, A., and Singh, H., 2011, "Optimization of processing parameters in induction hardening using response surface methodology", Indian academy of sciences, 36 (2), pp. 141–152.
[12] Hicks, C., 2009, "Fundamental Concepts in the Design of Experiments", Oxford Press, US.
[13] Lapin, L.L., 1998, "Probability and Statistics for Modern Engineering", PWS-KENT Publishing Company, Boston, US, Chap. 13.

Copyright © 2012 by ASME